Study of the Immersed Depth on the Natural Convection Heat Transfer from a Heated Triangular Prism Embedded in Porous Media

Suhad A. Rasheed

Lecturer
University of Technology
Mechanical Engineering Department
Baghdad
Iraq

Abdulsattar J. Hasan

Assistant Professor
University of Technology
Mechanical Engineering Department
Baghdad
Iraq

Estimating the heat loss encountered in many situations with a hot surface buried in a permeable material greatly contributes to the energy conservation and cost analysis of numerous engineering systems. An experimental study was conducted on the natural convection heat transfer from a triangular prism positioned in a 0.2 m^2 test section filled by 3 mm glass spheres as a porous material. The air is the working fluid used in the study with the Darcy-Raleigh number (0.1224≤ Ra* ≤ 0.2712). The triangular prism heater (having face side (c) = 0.026 m and L = 0.2 m) is made of copper that is heated electrically and immersed in the porous material at three different depth to radius ratios (h/R=3.5, 10, and 16.5). The results manifested that the peripheral surface temperature around the triangular prism rises with a rise in the h/R ratio and an increase in the heat flux. The mean Nusselt number is proportional to the heat flux and Darcy-Raleigh number. Empirical correlations were obtained from the experimental results, and the differences between measured and estimated values never exceeded ∓ 2.7.

Keywords: Natural convection, Immersed depth, Porous medium, Triangular cylinder, Crossflow

1. INTRODUCTION

The heat losses from embedded pipes and cylinders in a saturated porous medium have attracted substantial attention in the last few years. Such a problem gets up to practical importance in many engineering applications. Underground power transmission lines suffer from cable insulation failure due to the heat dissipation to the bedding soil, which would dry out depending on its water content. Cable overheating is inevitable, and the power transmission system's current carrying capacity and productivity are vulnerable to regression [1]. Oil and gas industries pay a great concern to the heat loss from the offshore buried pipelines in which convection through the sandy backfill soil is imminent. Crude oil encounters wax crystallization with a temperature drop when heavy components precipitate.

On the other hand, the natural gas would hydrate when combined with the free water under low temperature and high-pressure conditions [2]. District heating systems involving underground hot water distribution pipelines are subjected to damage caused by the heat transport to the cold surrounding bedding materials. Reducing the water temperature leads to a change in the density and viscosity of the water and freezing and flow blockage under sub-zero temperatures [3]. The heat generated by the nuclear wastes is released in a significant amount from a canister to the host rocks

at the final disposal sites. The resultant temperature distribution around these wastes is strongly affected by the rate of heat decay and the thermal properties of the buffer and the host rocks [4].

Ingham gave numerous publications in the field of the phenomenal porous media and Pop [6-8], Vafai [9,10], Bejan and Kraus [11], and Nield and Bejan [12]. Merkin [5] was the first who gave a correlation for natural convection from a horizontal cylinder immersed in a porous medium by experimental and analytical investigation. The natural convection heat transfer around an isothermal pipeline embedded in an infinite fluid-saturated porous medium was studied by Ingham and Pop [13] using various models. Nakayama and Koyama [14], Fand et al. [15], and Nakayama and Pop [16] obtained similar solutions for different horizontal, axisymmetric shapes. Fand et al. [17] experimentally investigated the natural convection from a horizontal cylinder crammed into glass spheres saturated by either silicone oil or water. The combined convection heat transfer from a horizontal cylinder embedded in a pack of glass spheres that were saturated with water in crossflow was studied by Fand and Phan [18].

Christopher and Wang [19] used the Fourier series method to solve the whole stream function and the equations of energy for 2D flow fields around a horizontal, isothermal cylinder in an infinite fluid-saturated porous medium. Atwan and Sakr[20] studied using the finite element method for a Darcy flow with a depth/radius ratio of 2≤ h/R ≤8. Yu et al. [21] investigated the transient natural convection numerically in an air-filled horizontal circular cylinder with a coaxial inner triangular cylinder for two different positions. Mohamed Ali and Nuhait [22] studied the

laminar forced convection heat transfer numerically around a horizontal triangular prism in the air under laminar conditions (Re ≤ 200) using the finite volume technique. A numerical study was conducted on the orientation of a heated triangular prism (flat side facing downward and upward) by Tiwari and Chhabra [23]. Hilal et al. [24] investigated the forced convection heat transfer of air in a porous rectangular duct.

A linear stability analysis was conducted to investigate the variable gravity effect on the onset of heat convection in a horizontal rotating nanofluid layer within a porous medium by Chand et al. [25]. The heat transfer from two isothermal offset square cylinders using a conjugate interface boundary was studied for a steady and periodic flow by Kanna et al. [26]. The simulation was carried out for Reynolds numbers varied from 10 to100 with a vortex onset at a Reynolds number of 48. Corasanitiand Gori [27] performed an experi–mental study concerning the natural convection of a vertical cylinder of a length/diameter ratio of 100 packed with 3 mm glass beads saturated by water. The desecrate Element Method (DEM) approach was emp–loyed to study the Packed-bed thermal energy storage (TES) behavior during a heating process by T. Mitterlehner et al. [28]. The walls of the heat-storage tank exerted increased stress due to the expansion of the thermal-storing medium. Abed et al. [29] investigated numerically the natural convection about a centered adiabatic circular cylinder inside a trapezoidal enclosure glutted with Ag–water nanofluid overlaying saturated porous–nanofluid layer using a finite element technique. Rasheed and Mahmood [30] studied theoretically and experimentally the natural convection from an electri–cally heated circular cylinder at various positions inside a square box with and without a porous medium at a fixed heat flux. Soltani-Tehrani et al. [31] investigated the effects of adding homogenous porous media to a wavy-tube heat exchanger. Ahamad et al. [32] studied the double diffusion within a square porous cavity subjected to conjugate heat transfer by the finite element method. Mohammed [33] investigated the laminar natu–ral convective heat transfer for air trapped between a heated inner equilateral triangular cylinder and an outer cold circular enclosure using Fluent CFD software.
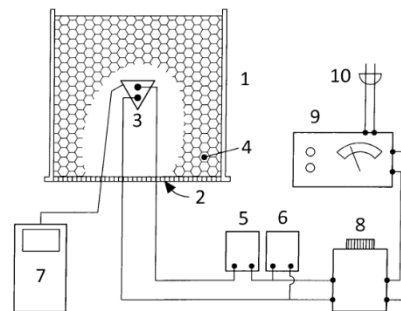
Despite that the concept of embedded bodies in porous media has been abundantly inspected over the last decades, most of these inspections have concerned the circular pipes and cylinders. There are still many situations in which polygonal bodies need to be investigated as a source of dispersing heat to an agglutinative domain. There are few studies concerning the natural heat transfer for triangular bodies placed in empty conduits rather than those packed with porous media. In that context, this work aims to study the natural convection heat transfer experimentally from a horizontal equilateral triangular prism placed in a square duct filled with glass spheres. The impact of varying the immersion depth of the prism on the heat transfer characteristics will be evaluated by the peripheral surface temperature and Darcy-Raleigh number. This effort is targeting to furnish a feasible approach to specify the best burial depth of the heat-dissipating sources in diverse engineering applications. The study

outcomes would reflect efficiently on the buried objects' lifetime and economic perspective via diminishing the maintenance and replacement costs.

2. EXPERIMENTAL SETUP

2.1 Apparatus and instrumentation

The test rig used in the study is mainly a square duct having 20 cm side length and 20 cm height and made of galvanized sheets, as depicted in figure (1). The duct walls are thermally insulated, and the air drought flows from the bottom to the top of the duct in a natural convection mode. The duct is packed with a porous medium consisting of 3 mm glass spheres to fill the entire volume of the duct between the bottom and the top sides. A metallic wire mesh is fixed at the bottom entry to prevent the downfall of the spheres due to gravity. The heating element is a triangular prism of 20 cm in length and a base-wide of 2.6 cm, giving a hydraulic diameter of 1.5 cm with the base facing upward. The prism, which is made of copper and heated internally by an electric heater of a 1 cm diameter and a 20 cm length, is inserted in a cross-through hole. Two rubber pieces are fixed at the prism's ends to prevent heat loss to the duct sides. The prism location concerning the duct's top end is allocated via three stations along the duct height to change the immersed depth to radius ratio (h/R), as manifested in figure (2).

1	Test section	6	Voltmeter
2	Mesh wire	7	Digital thermometer
3	Heated prism	8	Variac
4	Porous media	9	Stabilizer
5	Ammeter	10	Power supply

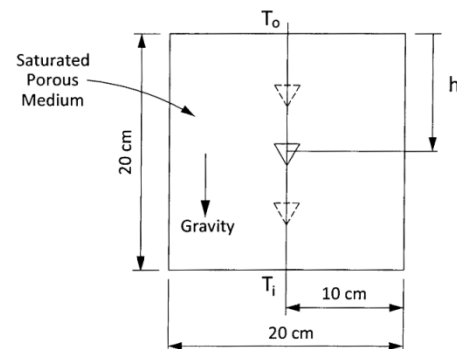**Figure 1. Schematic of the test rig**

Figure 2. Details of the test section

The surface temperature of the prism was measured by attaching three K-type thermocouples to each face of the triangle. Each thermocouple was inserted into a 1

mm slot at the surface, and it was separated from the other thermocouples by 5 cm [34], see figure (3). The temperature of the air drought at the entry and exit sections of the duct was measured using two more thermocouples installed at the center of these sections. All thermocouples were wired to a digital thermometer equipped with a selector switch to display one temperature at a time. The heating element is energized with AC-electric current via a 2000 W Dactrone voltage regulator, as viewed in figure (1). A variac type TDGC2 is linked to the voltage regulator to adjust the input voltage when required. The electric current and voltage were measured and displayed using a multimeter.
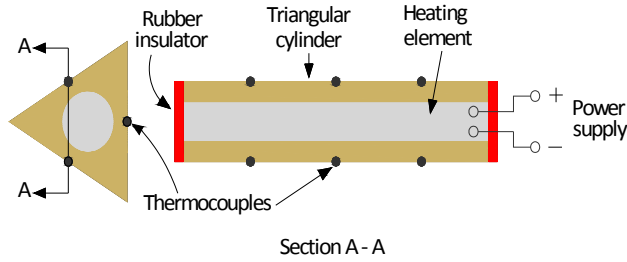

Section A - A

Figure 3. Thermocouples distribution around the prism [34]

The porosity ( ) was evaluated by measuring the volume of water needed to fill the voids between the particles in a prescribed vessel volume, and it was (0.389). The properties of the glass spheres used in the study are listed in Table 1. The comparable permeability was found to be 0.7884×10^{-8}m^2 as calculated byKozeny-Carmen equation [35]:

$$K = \frac{\varepsilon^3 d_p^2}{180(1-\varepsilon)^2} \qquad (1)$$

Table 1.The properties of the glass spheres [36]

Thermal conductivity	0.78 W/m^{o}C
Heat capacity	670 J/kg^{o}C
Density	2507 kg/m^3

2.2 Experimental procedure

The triangular prism was first fixed at the intended immersion depth (depth/radius ratio) before the test section duct was packed with the glass spheres up to the top edge of the duct. The constant heat flux was set at the desired value by supplying the heater with the corresponding voltage. Five values of heat flux (1282.051, 1038.462, 820.5128, 628.2051, and 461.5385 W/m^2) were chosen following the specified Darcy-Rayleigh number corresponding to the respective voltages (30, 35, 40, 45 and 50 volts). The data recording started after the steady-state of the whole system was reached, which has taken between 4-5 hours depending upon the desired heat flux.

3. PARAMETERS CALCULATION

The effective thermal conductivity of the porous medium was calculated using this mixing formula [30]:

$$K_m = \varepsilon K_f + (1-\varepsilon)K_s \qquad (2)$$

The mean air temperature is given by:

$$T_m = \frac{T_o + T_i}{2} \qquad (3)$$

The average surface temperature of the prism is:

$$T_w = \frac{\sum_{n=1}^{n=9} T_{wn}}{9} \qquad (4)$$

Now, the film temperature can be determined as:

$$T_f = \frac{T_m + T_w}{2} \qquad (5)$$

The total power supply to the prism heater is given by:

$$Q_t = I \times V \qquad (6)$$

Now, the net heat transfer was obtained by:

$$Q = Q_t - Q_{loss} \qquad (7)$$

The mean convective heat transfer coefficient was found by:

$$h_m = \frac{Q}{A_s(T_w - T_m)} \qquad (8)$$

A_s is the triangular prism surface area determined as (A_s = 3×c×L). Therefore, the mean Nu was calculated as:

$$Nu_m = \frac{h_m D_h}{K_m} \qquad (9)$$

The average surface temperature of the three ther–mocouples attached to each face of the triangular prism was determined as:

$$T = \frac{\sum_{n=1}^{n=3} T_{wn}}{3} \qquad (10)$$

From this, the local convective heat transfer coefficient was determined by:

$$h = \frac{Q}{A_s(T - T_m)} \qquad (11)$$

Also, the local Nusselt number is to be calculated as:

$$Nu = \frac{h D_h}{K_m} \qquad (12)$$

Another important parameter to be calculated is the Darcy-Rayleigh number:

$$Ra^* = \frac{g\beta K R(T_w - T_m)}{\alpha \nu} \qquad (13)$$

where β is given by the expression:

$$\beta = \frac{1}{T_f} \qquad (14)$$

To verify the mean Nusselt number obtained in this study, the correlation obtained analytically by Merkin [5]around a circular cylinder is:

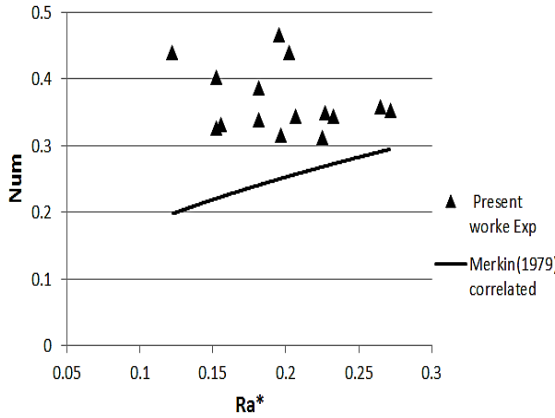$$Nu_m = 0.565\,Ra^{*0.5} \qquad (15)$$

Figure 4. Comparison between the experimental and the estimated mean Nusselt number [5]

This equation will be compared with the current experimental values for the triangular prism, which has the same hydraulic diameter of 1.5 cm, as in [5]. The comparison is illustrated in figure (4), and the average deviation was found to be $\mp12\%$. A similar trend for both the cases is evident in the figure as the mean Nusselt number increases with the increase in Darcy-Rayleigh number within the range $0.1224 \leq Ra^* \leq 0.2712$ and the extent of agreement obtained is reasonable.

4. RESULTS AND DISCUSSION

The present work is devoted to studying the effect of the immersion depth/radius (h/R) ratio on the natural convection heat transfer characteristics from a heated triangular prism embedded in a porous medium. The layout of the prism concerning the direction of gravity and the locations of the measuring points of the peripheral surface temperature are demonstrated in figure (5).
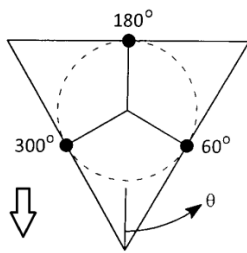

Figure 5. Angular locations of thermocouples and gravity direction.

Figure (6) portrays the relationship between the average face temperature of the prism and the angular locations shown in figure (5) at a depth/radius ratio of 16.5. The local peripheral temperature around the prism surfaces is constant at a given value of heat flux, yet, it is increased by increasing the heat flux from 30 V to 50 V by 18.6%. This is attributed to the increase in the energy dissipated at the higher heat flux with a given cooling potential set by the configuration of the test section under the natural convection mode. For the same rise in heat flux, the increase in the peripheral temperature reaches 18.2% for a depth/radius ratio of 10

in figure (7), while it becomes 18.3% in figure (8) for a depth/radius ratio of 3.5.
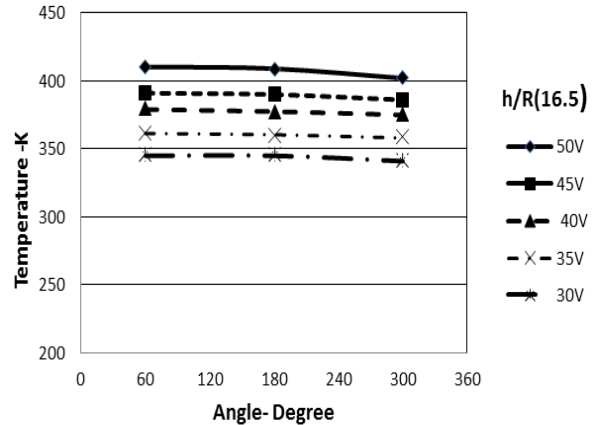

Figure 6.Average face temperature with different voltages at a depth/radius ratio of 16.5.
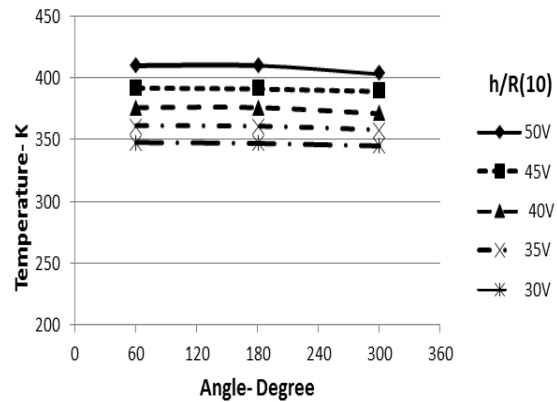

Figure 7. Average face temperature with different voltages at a depth/radius ratio of 10.
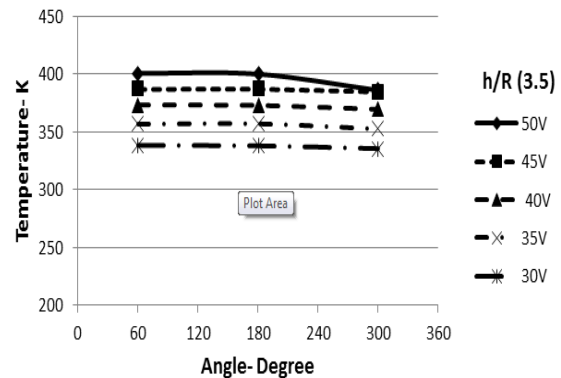

Figure 8. Average face temperature with different voltages at a depth/radius ratio of 3.5.

The local Nusselt number around the perimeter of the prism is almost fixed due to the shape symmetry, as presented by figure (9) for a depth/radius ratio of 10. On the other hand, this local Nusselt number increases with the increase in heat flux, which follows the convective heat transfer coefficient. The percentage increase in the local Nusselt number is 8.2% when the heat flux increases from 461.5385 W/m^2 to 1282.051 W/m^2, corresponding to the respective increase from 30 V to 50 V. This is ascribed to the fact that the increment in the heat flux exceeds the heat associated with the rise in temperature difference between the surface and the fluid $(q/(T_w - T_\infty))$.
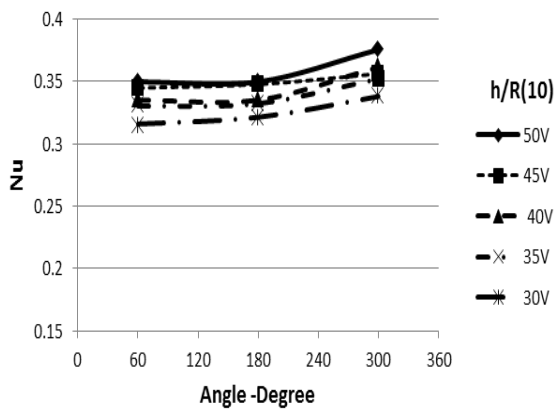
Figure 9. Local Nu with different voltages at a depth/radius ratio of 10.

Figure (10) elucidates that the local temperature at a constant heat flux of (1282.051 W/m^2) is approximately constant around the prism but only increases with the depth/radius ratio increase. The ratio of 3.5 gives a better cooling since the heater is closer to the upper side of the packed enclosure. Nevertheless, the other two locations are deeply immersed into the porous medium in regions with weak convection, especially at the triangle base, where the conduction through the medium is dominated. This location helps enhance the con–vective currents developed and carry the heat to the close ambient air at the upper side.
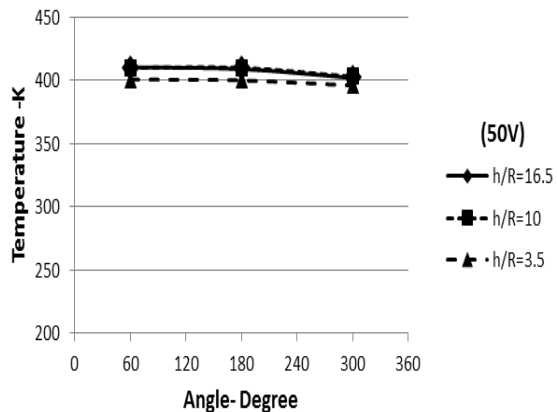

Figure 10. Average face temperature with different depth/radius ratios at a voltage of 50 V.

Figures (11) and (12), at the respective constant heat fluxes 1282.051 and 628.205 W/m^2, comply with the outcomes of figure 10 in which the best cooling takes place at a depth/radius ratio 3.5. More cooling leads to a larger temperature difference and a higher convective heat transfer coefficient. Therefore the local Nusselt number is the highest at a depth/radius ratio of 3.5. As depicted in figure (11), at a heat flux of 1282.051 W/m^2, the achieved enhancement is 40% in the local Nusselt number when the ratio of depth/radius is changed from 16.5 to 3.5. Nevertheless, at a heat flux of 628.205 W/m^2, the obtained enhancement in the local Nusselt number is only 16.8%, accompanying the change in the depth/radius ratio from 16.5 to 3.5, as exhibited in figure (12).

The relation between the mean heater surface temperature and the heat flux is depicted in figure (13). It denotes the direct proportionality of the temperature

with increasing heat flux. It is evident from the figure that the maximum recorded increase in the mean temperature is 3% when raising the ratio of depth/radius from 3.5 to 16.5 at a higher heat flux of 1282.051 W/m2. This is expected as higher heat flux means more energy to dissipate within the prism material. As the heat flux increases from 461.5385 W/m^2 to 1282.051 W/m^2, the prism means the surface temperature is augmented by 16.4%, 17.6%, and 18.6% for a depth/radius ratio 3.5, 10, and 16.5, respectively. Also, this figure suggests that the increase in temperature with increasing depth/radius is attributed to the more porous material stacked above the prism, which obstructs the heat transfer by convection.
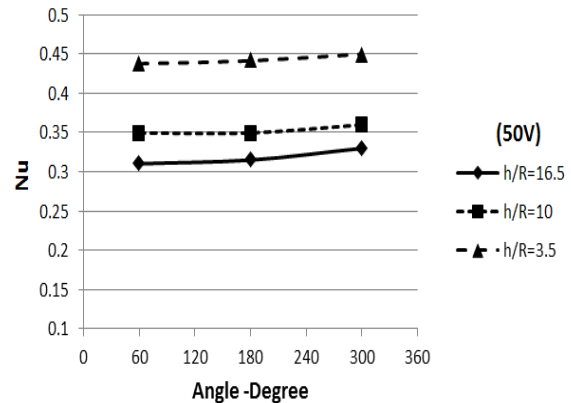

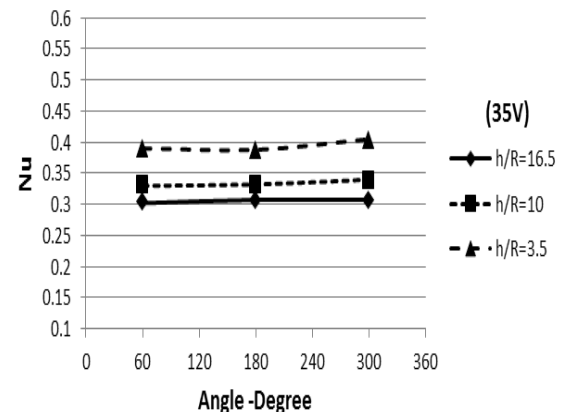**Figure 11. Local Nu with different depth/radius ratios at 50 V (1282.051 W/m^2).**

Figure 12. Local Nu with different depth/radius ratios at 35 V (628.051 W/m^2).
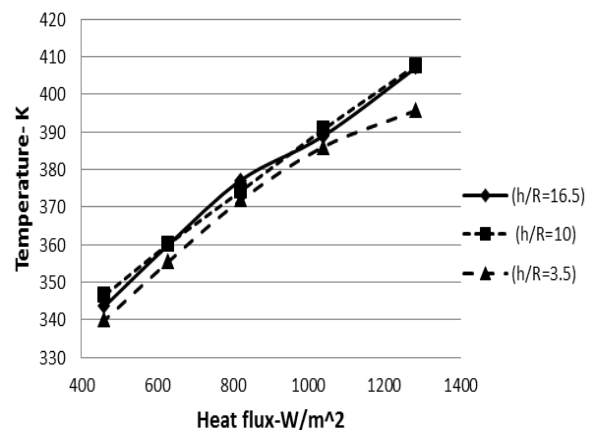

Figure 13. Mean surface temperature versus heat flux with different depth/radius ratios.

Generally, the same trend as that in figure (13) is realized with the Nusselt number shown in figure (14) revealing the direct proportionality with increasing the heat flux from 461.5385 W/m^2 to 1282.051 W/m^2. The percentage increase in the mean Nusselt number is 15.6%, 10.3%, and 10% for the respective depth/radius ratios of 3.5, 10, and 16.5. The lower surface tempe–rature resulting from the heat dissipation to the nearer ambient air at the upper side will certainly enhance the convective cooling and increase the Nusselt number.
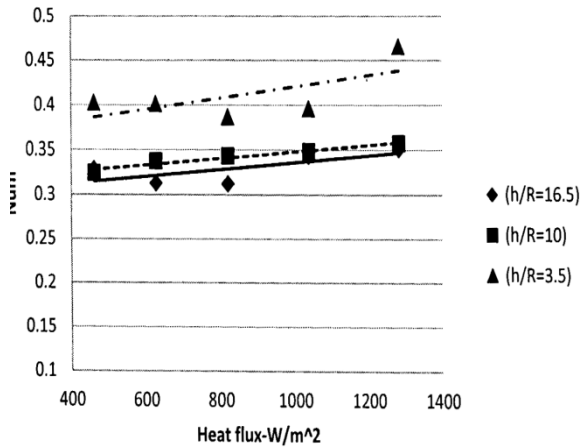

Figure 14. Mean Nu versus heat flux with different depth/radius ratios.

Figure (15) manifests the relationship between the mean Nusselt number and the Darcy-Rayleigh number for the immersion depth/radius ratios considered in the study. It is observed that the increase in the mean Nusselt number with the Darcy-Rayleigh number de–pends on the selected value of the depth/radius ratio. For the ratios of 10 and 16.5, the Darcy-Rayleigh number increased in the range $0.153 \leq Ra^* \leq 0.27$, with a corresponding increase in the mean Nusselt number of 10.3%. Nevertheless, at the ratio of 3.5 for the range $0.1224 \leq Ra^* \leq 0.202$, the mean Nusselt number increase only reached 6.3%, as appears in figure (15). The increase in the Darcy-Rayleigh number brings a higher convection heat transfer from the prism surface to the air and creates two counter-rotating vortices at the sides of the prism, which are rising upwards. The convective heat transfer coefficient will increase with the Darcy-Rayleigh number due to the thinning of the boundary layer that accompanies the increase in air velocity [21]. At a Darcy-Rayleigh number of 0.153, the value of the mean Nusselt number is 0.4017, 0.3244, and 0.33 at the depth/radius ratios of 3.5, 10, and 16.5, respectively. It is clear that the higher Nusselt number is obtained at the ratio of 3.5, because the effects of the natural convection vortices are stronger, and the velocity is higher at that location as the prism is close to the upper side of the duct, which is open to the ambient air. Additionally, at the lowest location with the ratio of 16.5, the vortices are rotating and dissipating heat to the open bottom side of the duct as well. However, at the central location with the depth/radius ratio of 10, the effect of vortices is weaker and far from both open sides of the duct.

According to the experimental data explored in figure (15), correlated equations were obtained relating

the Darcy-Rayleigh number with the mean Nusselt number. They are listed in Table (2) for the different depth/radius ratios.
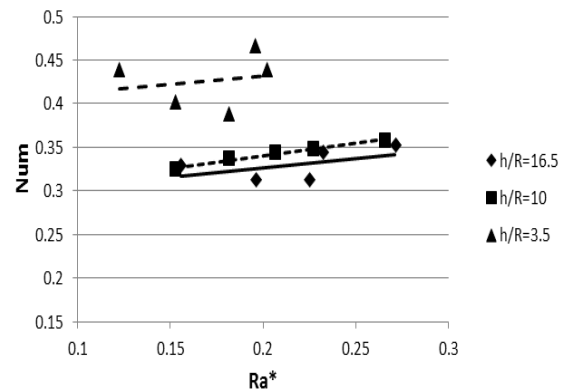

Figure 15. Mean Nu versus Ra* with different depth/radius ratios.

Table 2. The correlation equations

h/R	Correlations
3.5	$Num = 0.466 Ra*^{0.0507}$
10	$Num = 0.4506 Ra*^{0.1726}$
16.5	$Num = 0.3976 Ra*^{0.1212}$

5. EMPIRICAL CORRELATIONS OF THE PRESENT WORK

According to the experimental results obtained throughout the study, a regression analysis was used to find a relationship between the key parameters (Rayleigh number and the immersion depth/radius ratio). The intended empirical correlation is given by:

$$Nu_m = 0.3794 Ra*^{-0.163} (h/R)^{-0.146} \qquad (16)$$

Equation 16 is applicable within $0.1224 \leq Ra^* \leq 0.2712$ and the depth/radius ratios of 3.5, 10, and 16.5. The mean Nusselt number and Darcy-Rayleigh number were calculated based on the hydraulic diameter of the prism.

Figure (16) appears the graphical presentation of the obtained correlation, which is superimposed on the experimental data extracted under the varying conditions of the study. A comparison between the correlated values of the mean Nusselt number from equation 16 and the measured values is shown in figure (17), in which the average deviation never exceeds ($\pm 2.7\%$).
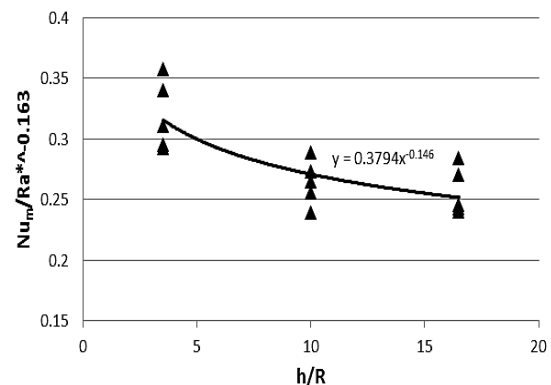

Figure 16. Relation between (Nu$_m$/Ra$^{*-0.163}$) and depth/radius ratio.
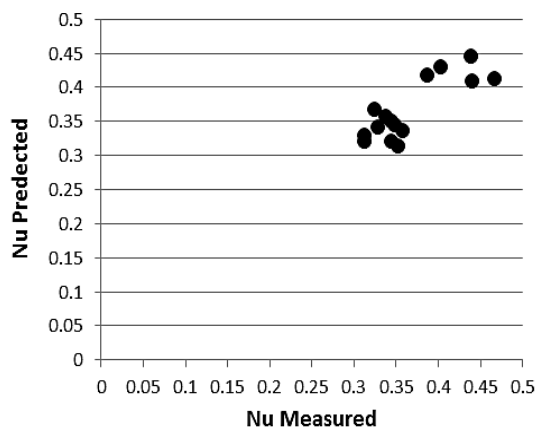
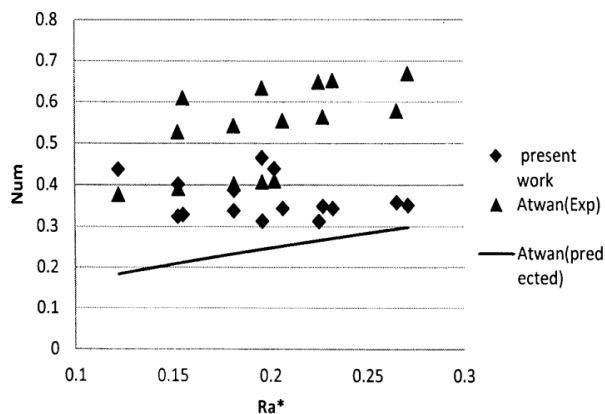**Figure 17. Relation between predicted and measured Nu.**

Figure 18.Comparison between the present work and the results of Atwan et al. [20].

6.   COMPARISON WITH PREVIOUS WORK

Figure (18) compares the experimental results of the present work and the experimental results obtained from the correlated equation suggested by Atwan et al. [20] for a circular cylinder embedded in the sand with grains having a 2.7 mm diameter. The general similarity in the trends of both works is obvious and within acceptable limits. The difference in the immersed body configurations and the ranges of Darcy-Rayleigh number caused a slight deviation in the figure. The average deviation observed is ($\pm14\%$) between the present work and the correlated results of [20].

7.   CONCLUSION

The following conclusions can be drawn from the results of studying the effect of the immersion depth/radius ratio on the characteristics of natural convection from a triangular prism immersed in a porous medium:

*   The local peripheral temperature increases with increasing the depth/radius ratio, and the ratio of 3.5 gives the best cooling characteristic.
*   The mean surface temperature is directly proportional to the heat flux, increasing with the increase in the depth/radius ratio.
*   The local Nusselt number increases with the increase in heat flux due to the convective heat transfer coefficient.

*   The mean Nusselt number is directly proportional to the Darcy-Rayleigh number and is inversely proportional to the depth/radius ratio, increasing the resistance to the convective heat transfer.
*   The deviation between the predicted and the experimental values never exceeded ± 2.7%, as given by the empirical correlation obtained.

REFERENCES

[1] Verschaffel-Drefke, C., Schedel, M., Balzer, C., Hinrichsen, V. and Sass, I.: Heat dissipation in variable underground power cable beddings: Experiences from a real scale field experiment, Energies, Vol. 14,2021, 7189. https://doi.org/ 10.3390/en14217189.

[2] Chakraborty, S.: Experimental investigation and modeling of heat loss mechanism from offshore buried pipelines, M.Sc. Thesis, Faculty of Engineering and Applied Science, Memorial University of Newfoundland, 2017.

[3] Pavel Sláma, P. and Nožička, J.: Heat loss Calculations of Underground Central Heating Pipelines, Acta Mechanica Slovaca, Vol. 22, No. 2, pp. 48-53, 2018.

[4] Yanga, S. and Yeh, H.: Modelling transient heat transfer in nuclear waste repositories, Journal of Hazardous Materials, Vol. 169, pp. 108–112, 2009.

[5] Merkin, J.H.: Free convection boundary layers on axisymmetric and two-dimensional bodies of arbitrary shape in a saturated porous medium, International Journal of Heat and Mass Transfer, Vol. 22, pp. 1461-1462, 1979.

[6] Ingham, D.B. and Pop, I.: *Transport Phenomena in Porous Media*, Vol. I, Pergamon, Oxford, 1998.

[7] Ingham, D.B. and Pop, I.: *Transport Phenomena in Porous Media*, Vol. II, Pergamon, Oxford, 2002.

[8] Ingham, D.B. and Pop, I.: *Transport Phenomena in Porous Media*, Vol. III, Pergamon, Oxford. 2005.

[9] Vafai, K.: Handbook of Porous Media, Vol. I, Marcel Dekker, New York, NY, 2000.

[10] Vafai, K.: Handbook of Porous Media, Vol. II, Marcel Dekker, New York, NY. 2005.

[11] Bejan, A. and Kraus, A.D.: *Heat Transfer Handbook*, Wiley, New York, NY, 2003.

[12] Nield, D.A. and Bejan, A.: Convection in Porous Media, 3rd ed., Springer, Berlin, 2005.

[13] Ingham, D.B. and Pop, I.: Natural convection about a heated horizontal cylinder in a porous medium, Journal of Fluid Mechanics, Vol. 184, pp.157-181, 1987.

[14] Nakayama, A., Koyama, H.: Free connective heat transfer over a non-isothermal body of arbitrary shape embedded in a fluid saturated porous medium, Journal of Heat Transfer, Vol. 109, pp.125-130, 1987.

[15] Fand, R. M., Steinberger, T. E. and Cheng, P.: Natural convection heat transfer from a horizontal cylinder embedded in a porous medium, International Journal of Heat and Mass Transfer, Vol. 29, pp.119-133, 1986.

[16] Nakayama, A. and Pop, I.: A unified similarity transformation for free, forced and mixed convection in Darcy and non-Darcy porous media, International Journal of Heat and Mass Transfer, Vol. 34, pp.357-367, 1991.

[17] R.M.F., Steinberger, T.E.and Cheng, P.: Natural convection heat transfer from a horizontal cylinder embedded in a porous medium Convection, International Journal of Heat and Mass Transfer, Vol. 29, Issue 1, pp. 119-133, 1986.

[18] Fand, R.M.and Phan, R.T.: Combined forced and natural convection heat transfer from a ho–rizontal cylinder embedded in a porous me–dium, International Journal of Heat and Mass Transfer, Vol. 30, Issue 7, pp.1351-1358, 1987

[19] Christopher, D.M. andWang, B.X.: Natural convection around a horizontal cylinder in a fluid-saturated porous media using Fourier series, Trans. on Engineering Sciences, Vol. 5, pp. 427-434, WIT Press, 1994.

[20] Atwan, E. F., Sakr, R.Y.: Natural convection heat transfer from a heated pipe embedded in a liquid-saturated porous medium", Engng. Res. Jour., Vol. 98, pp. M52-M69, Helwan Univer–sity, Faculty of Engineering, Mataria, Cairo, 2005.

[21] Yu Z. et al.: Transient natural convective heat transfer from a heated triangular cylinder to its air-filled coaxial cylindrical enclosure, International Journal of Heat and Mass Transfer, Vol. 53, pp.4296–4303, 2010.

[22] Mohamed Ali, O.Z., Nuhait, A.: Convective heat transfer around a triangular cylinder in an air cross flow, International Journal of Thermal Sciences, Vol. 50, Issue 9, pp. 1685-1697, 2011.

[23] Tiwari, A.K., Chhabra R. P.: Effect of orient–tation on the steady laminar free convection heat transfer in power-law fluids from a heated triangular cylinder, Numerical Heat Transfer, Part A, Vol. 65, pp. 780–801, 2014.

[24] Hilal, K. H., Saleh, A.M. and Ebraheem, M.H.: An experimental study on heat transfer enhancement for porous heat exchange in rectangular duct, Eng. & Tech. Journal, Vol.32, Part (A), No.11, pp. 2788-2802, 2014.

[25] Chand, R., Rana, G. C., Kango, S. K.: Effect of Variable Gravity on Thermal Instability of Rotating Nanofluid in Porous Medium, FME Trans., Vol. 43, pp.62-69, 2015.

[26] [26]Kanna, P.R., Sivasubramanian, M. and Uthayakumar, M.: Numerical Investigation of ForcedConvection Heat Transfer from Square Cylinders in a Channel Covered by Solid wall - Conjugate Situation, FME Trans., Vol. 45, pp.16-25, 2017.

[27] Corasaniti, S. and Gori, F.: Natural convection around a vertical cylinder (thermal probe) immersed in a porous medium, International Communications in Heat and Mass Transfer, Vol. 81, pp. 72–78, 2017.

[28] Mitterlehner, T., Kartnig, G. and Haider, M.: Analysis of the Thermal Ratcheting Pheno–menon in Packed-bed Thermal Energy Storage using Discrete Element Method, FME Trans., Vol. 48, pp. 427-431, 2020.

[29] Abed, I. M., Abdulkadhim, A., Hamzah R. A., Hamzah, H. K., Ali F. H.: Natural convection heat transfer for adiabatic circular cylinder inside a trapezoidal enclosure filled with nano–fluid superposed porous–nanofluid layer, FME Trans., Vol.48, pp.82-89, 2020.

[30] Rasheed, S. A., Mahmood, A.A.:Free convec–tion heat transfer around a cylinder embedded in an enclosure filled with porous media, Al-Nahrain Journal for Engineering Sciences, Vol.23, Part 1, pp. 51-60, 2020

[31] Soltani-Tehrani, A., Tavakoli, M. R., Salim–pour, M. R.:Using porous media to improve the performance of a wavy-tube heat exchanger, FME Trans., Vol. 46, No. 4, pp. 631-635,2018.

[32] Ahamad,N.A.,Kamangar, S., Aljohani,A. F., Azeem, Baig, M.A., and Badruddin, I. A.: Double diffusion in square porous cavity subjected to conjugate heat transfer, FME Trans., Vol. 48, pp. 841-848, 2020.

[33] Mohammed, A.A.: Natural convection heat transfer inside horizontal circular enclosure with triangular cylinder at different angles of inclination, Journal of Thermal Engineering, Vol. 7, No. 1, pp. 240-254, 2021

[34] Rasheed, S. A.: Enhancement in forced convection heat transfer from a heated triangular cylinder by using porous media"Journal of Mechanical Engineering Research and Developments, Vol. 44, No. 1, pp. 135-150, 2021.

[35] Nield D. A., Kuznetstov: Forced convection in a Bi-disperse porous medium channel, Int. Jour. of Heat and Mass Transfer, Vol. 47, pp. 5375-5380, 2004.

[36] Holman J.P.: Heat transfer, McGraw-Hill, New York, 2010.

NOMENCLATURE

A The cross-sectional area of test section (m^2)
A_s Surface area of the triangular prism (m^2)
C_p Specific heat (J/kg.^{o}C)
D_h Hydraulic diameter of triangular cylinder (m)
c The side length of triangular cylinder (m)
h Local heat transfer coefficient (W/m^2.^{o}C)
h_m Average heat transfer coefficient (W/m^2.^{o}C)
I Current (Amp)
K Thermal conductivity (W/m.^{o}C)
Nu Local Nusselt number
Nu_m Mean Nusselt number
$Ra*$ Darcy-Raleigh number

T	Temperature (K)
Q_t	Total power supply to the heater (W)
V	Voltage (Volt)

Greek symbols

	Porosity (-)
ρ	Density (kg/m³)
β	Volume coefficient of expansion

Subscripts

a	Air
i	Inlet
o	Outlet
m	Effective
f	Fluid
s	Solid

ПРОУЧАВАЊЕ ДУБИНЕ УРОЊЕЊА НА ПРИРОДНИ КОНВЕКЦИЈСКИ ПРЕНОС ТОПЛОТЕ ИЗ ЗАГРЕЈАНЕ ТРОУГЛАСТЕ ПРИЗМЕ УГРАЂЕНЕ У ПОРОЗНЕ МЕДИЈЕ

С.А. Рашид, А.Џ. Хасан

Процена топлотног губитка који се јавља у многим ситуацијама са врелом површином закопаном у пропусни материјал у великој мери доприноси уштеди енергије и анализи трошкова бројних инжењерских система. Експериментално истражи– вање је спроведено о природном конвекцијском преносу топлоте са троугласте призме постављене у испитни део од 0,2 м2 испуњен стакленим сферама од 3 мм као порозним материјалом.

Ваздух је радна течност коришћена у студији са Дарси-Релијевим бројем (0,1224≤ Ra* ≤ 0,2712). Грејач троугласте призме (с предњом страном (ц) = 0,026 м и Л = 0,2 м) је направљен од бакра који се загрева електричним путем и потапа у порозни материјал на три различита односа дубине и радијуса (x/P=3,5, 10, и 16.5). Резултати су показали да температура периферне површине око троугласте призме расте са порастом x/P односа и повећањем топлотног флукса. Средњи Нуселтов број је пропорционалан топлотном флуксу и Дарци-Ралеигховом броју. Из експерименталних резултата добијене су емпиријске корелације, а разлике између измерених и процењених вредности никада нису прелазиле ±2,7.